

Identification of the Proteasome Inhibitor MG262 as a Potent ATP-Dependent Inhibitor of the *Salmonella enterica* serovar Typhimurium Lon Protease[†]

Hilary Frase, Jason Hudak, and Irene Lee*

Department of Chemistry, Case Western Reserve University, Cleveland, Ohio 44106

Received March 17, 2006; Revised Manuscript Received May 12, 2006

ABSTRACT: Lon is a homo-oligomeric ATP-dependent serine protease which functions in the degradation of damaged and certain regulatory proteins. The importance of Lon activity in bacterial pathogenicity has led to its emergence as a target in the development of novel antibiotics. As no potent inhibitors of Lon activity have been reported to date, we sought to identify an inhibitor which could serve as a lead compound in the development of a potent Lon-specific inhibitor. To determine whether a nucleotide- or peptide-based inhibitor would be more effective, we evaluated the steady-state kinetic parameters associated with both ATP and peptide hydrolysis by human and *Salmonella enterica* serovar Typhimurium Lon. Although the ATP hydrolysis activities of both homologues are kinetically indistinguishable, they display marked differences in peptide substrate specificity. This suggests that a peptide-based inhibitor could be developed which would target bacterial Lon, thereby decreasing side-effects due to cross-reactivity with human Lon. Using *Salmonella enterica* serovar Typhimurium Lon as a model, we evaluated the IC₅₀ values of a series of commercially available peptide-based inhibitors. Those inhibitors which behave as transition state analogues were the most useful in inhibiting Lon activity. The peptidyl boronate, MG262, was the most potent inhibitor tested (IC₅₀ = 122 ± 9 nM) and required binding, but not hydrolysis, of ATP to initiate inhibition. We hope to use MG262 as a lead compound in the development of future Lon-specific inhibitors.

The number of pathogenic, antibiotic-resistant bacteria increases each year; however, the development of new antibiotics to treat them lags behind (1). Recent studies aimed at identifying proteins necessary for virulence have implicated the importance of Lon protease (2, 3). Pathogenic *Salmonella enterica* are responsible for causing a range of human diseases from mild gastroenteritis (serovar Typhimurium and serovar Enteritidis) to typhoid fever (serovar Typhi). It has been demonstrated that *Salmonella enterica* serovar Typhimurium (*S. Typhimurium*) Lon protease activity is required for systemic infection in mice, a common study model for *S. Typhi* infection in humans (3). In fact, Lon-deficient *S. Typhimurium*, when administered as an oral vaccine to mice, conferred subsequent protection against infection by virulent *S. Typhimurium* (4). Taken together, these studies highlight Lon as an important target in the development of novel therapeutic agents.

Lon, also known as the protease La, is a homo-oligomeric ATP-dependent serine protease, which functions in the degradation of damaged and certain short-lived regulatory proteins (5–14). Homologues exist ubiquitously in nature; however, they localize to the cytosol in prokaryotes and to the mitochondrial matrix in eukaryotes (8, 15, 16). Sequence alignment of the human, *Escherichia coli* (*E. coli*), and *S. Typhimurium* Lon proteases has revealed that the bacterial enzymes share greater than 99% sequence identity, but only

42% identity with their human homologue (17). In fact the *E. coli* and *S. Typhimurium* Lon proteases differ in only three amino acids, none of which occur within the functional domains of the enzyme, indicating the two may function comparably. This is supported by the fact that Lon-deficient *E. coli* and *S. Typhimurium* are indistinguishable in their increased sensitivity to UV light and other DNA damaging agents, as well as their decreased ability to degrade abnormal proteins (11, 18–23).

Lon protease is a member of the AAA⁺ superfamily (ATPases Associated with different cellular Activities) along with other ATP-dependent proteases such as ClpXP, HslUV, and the proteasome (24, 25). These proteins all share a common ATPase domain consisting of the Walker A and B motifs. Both Lon and HslUV, the bacterial homologue of the proteasome, undergo a conformational change upon ATP binding (26, 27). Crystallographic studies of a truncated Lon mutant have suggested that Lon utilizes a Ser–Lys dyad to catalyze proteolysis, similar to the Thr–N terminal amino group dyad used by the proteasome (28, 29). Furthermore, both Lon and the proteasome are susceptible to serine protease, as well as cysteine protease inhibitors (30–33). As such, we hypothesize that approaches useful in developing inhibitors of proteasome activity may also be useful in developing inhibitors of bacterial Lon activity.

Although both nucleotide- and peptide-based inhibitors of Lon protease have been evaluated (30–32), none are highly potent or specific. Also, no detailed quantitative analysis has been done to allow comparison of these inhibitors. In this study, we aimed to quantitatively identify an inhibitor which could serve as a lead compound in the development of a

[†] This work was supported by the NIH Grant GM067172. J.H. is the recipient of the SPUR fellowship, a program sponsored by the Howard Hughes Medical Institute.

* Corresponding author. Phone, 216-368-6001; e-mail, irene.lee@case.edu; fax, 216-368-3006.

potent Lon-specific inhibitor. We evaluated the steady-state kinetic parameters associated with both ATP and peptide hydrolysis by human and *S. Typhimurium* Lon. Although the ATP hydrolysis activities of both homologues are kinetically indistinguishable, they display differences in their substrate specificity. This suggests that a peptide-based inhibitor could be designed which would target bacterial Lon, thereby decreasing side-effects due to cross-reactivity with human Lon. Using *S. Typhimurium* Lon as a model, we evaluated the IC_{50} values of a series of commercially available peptide-based proteasome inhibitors. We have identified the peptidyl boronate, MG262, as a potent ATP-dependent inhibitor of *S. Typhimurium* Lon activity ($IC_{50} = 122 \pm 9$ nM).

MATERIALS AND METHODS

Materials. All oligonucleotide primers were purchased from Integrated DNA Technologies, Inc. (Coralville, IA). All cloning reagents were purchased from Promega (Madison, WI), New England BioLabs, Inc. (Ipswich, MA), Invitrogen (Carlsbad, CA), and USB Corporation (Cleveland, OH). Fmoc-protected¹ amino acids, Boc-2-Abz-OH, Fmoc-Lys(Aloc)-Wang resin, Fmoc-Leu-Wang resin, Z-Leu-OSu, and HBTU were purchased from Advanced ChemTech and NovaBiochem. MG262, epoxomicin, and ZL₃VS were purchased from Biomol International, LP. MG132 was purchased from BostonBiochem. Tris buffer, cell culture media, IPTG, chromatography media, DTT, Mg(OAc)₂, trypsin, kanamycin, ATP, AMPPNP, ethylboronic acid, isopropylboronic acid, DMSO, SDS, and EDTA were purchased from Fisher, Sigma, and Amresco (Solon, OH).

Plasmid Construction. The *S. Typhimurium* Lon gene was amplified from genomic DNA (a gift from D. Kehres in M. Maguire's lab at Case Western Reserve University School of Medicine) using the oligonucleotides 5'-TAATACCCATGGGGAATCCTGAGCGTTCTGAA-3' and 5'-AAACCCAAGCTTCTACTATTGCGGTTACAACCT-3'. The resultant PCR product was cloned into the NcoI and HindIII sites of pET24d(+) (Novagen) to create the plasmid pHF020. The NdeI-BamHI fragment from proEx-1/hLon (34) was cloned into pET24c(+) (Novagen) to create the plasmid pHF002. Both plasmids express the mature wild-type enzymes without any exogenous tags and were verified by DNA sequencing. Our *S. Typhimurium* Lon gene harbors a naturally occurring conservative mutation, V378I, which does not occur within the functional domains.

Purification of Recombinant Lon. Recombinant *S. Typhimurium* Lon was overexpressed in BL21 (DE3) (Novagen), using the plasmid pHF020, and purified as previously

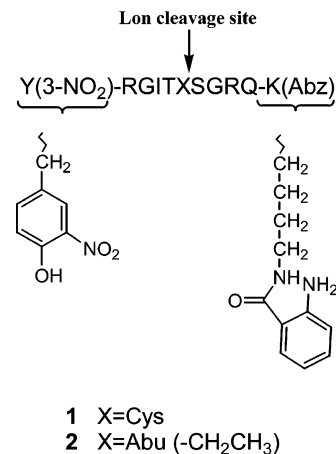


FIGURE 1: Substrates for continuous fluorescent measurement of Lon peptide cleavage. Upon Lon cleavage between X and S, an increase in fluorescence is observed as the fluorophore, K(Abz) (lysine anthranilamide), and quencher, Y(3-NO₂) (3-nitrotyrosine), separate. In the nonfluorescent analogues, the Y(3-NO₂) is replaced by Y and the K(Abz) is replaced by K(Bz) (lysine benzoic acid amide).

published for *E. coli* Lon (35) with the exception that 30 μ g/mL Kan (Sigma) was used instead of 100 μ g/mL Amp (Fisher). Recombinant human Lon was overexpressed in Rosetta (DE3) (Novagen), using the plasmid pHF002, and purified as described previously (36) with the following modifications. Following fractionation on a P11 column, the human Lon-containing fractions were pooled and precipitated using saturated ammonium sulfate. The precipitate was recovered by centrifugation and resuspended in Solution A (36), containing 2 mM DTT instead of 2 mM β -mercaptoethanol, and fractionated on a Superose 6 (Pharmacia) gel filtration column equilibrated in the same buffer. The concentration of Lon monomer was determined by Bradford assay, using BSA as a standard, and the purified protein was stored at -80°C .

Peptide Synthesis. Synthesis of **1**, **2**, ZL₃OH, and the corresponding nonfluorescent analogues of **1** and **2** (Figure 1) were performed as previously described (35).

Continuous Steady-State Peptide Hydrolysis Assay. Steady-state velocity data were collected on a Fluoromax 3 spectrophotometer (Horiba Group) as previously described for *E. coli* Lon (35) with the following modifications. All reactions contained 50 mM Tris (pH 8.1), 10 mM Mg(OAc)₂, 2 mM DTT, 150 mM NaCl (human Lon reactions only), 125–200 nM *S. Typhimurium* Lon monomer or 900 nM human Lon monomer, and varying concentrations of the peptide substrate (from 0 to 3.5 mM). At peptide concentrations between 100 μ M and 1 mM, a mixture of 10% fluorescent peptide and 90% of the corresponding nonfluorescent analogue was used to avoid the inner filter effect. Likewise, at peptide concentrations greater than 1 mM, a mixture of 1% fluorescent peptide and 99% of the corresponding nonfluorescent analogue was used to avoid the inner filter effect. After equilibration at 37°C for 1 min, the reaction was initiated by the addition of 1 mM ATP. The steady-state velocities were determined from the linear phase of the reaction time courses using KaleidaGraph (Synergy, Inc.). The steady-state kinetic parameters associated with peptide cleavage were determined by fitting the k_{obs} data with

¹ Abbreviations: ATP, adenosine triphosphate; AMPPNP, adenosine 5'-(β , γ -imino)triphosphate; ADP, adenosine diphosphate; KPi, potassium phosphate; DTT, dithiothreitol; Abz, anthranilamide; Bz, benzoic acid amide; Abu, 2-aminobutyric acid; 3-NO₂, 3-nitro; Aloc, allyloxycarbonyl; OSu, *N*-hydroxysuccinimide ester; HBTU, *O*-benzotriazole-*N,N'*,*N'*-tetramethyl-uronium-hexafluoro-phosphate; GST, glutathione *S*-transferase; Tris, 2-amino-2-(hydroxymethyl)-1,3-propanediol; Mg(OAc)₂, magnesium acetate; Fmoc, 9-fluorenylmethoxycarbonyl; Boc, butoxycarbonyl; PEI, polyethyleneimine; Z, *N*^α-benzyloxycarbonyl; ZL₃VS, *N*^α-benzyloxycarbonyl-L-leucyl-L-leucyl-L-leucyl-L-leucyl vinyl sulfone; ZL₃OH, *N*^α-benzyloxycarbonyl-L-leucyl-L-leucyl-L-leucine; SDS, sodium dodecyl sulfate; DMSO, dimethyl sulfoxide; EDTA, ethylenediaminetetraacetic acid; Amp, ampicillin; Kan, kanamycin; dlu, density light unit.

eq 1 using the nonlinear regression program Prism 4 (GraphPad Software, Inc.).

$$k_{\text{obs}} = \frac{k_{\text{cat}}[\text{S}]}{K_m^n + [\text{S}]^n} \quad (1)$$

where k_{obs} is the observed rate constant, k_{cat} is the maximal k_{obs} , S is peptide substrate, n is the Hill coefficient, and K_m is the Michaelis-Menten constant. All experiments were performed at least in triplicate.

Radiolabeled ATP Hydrolysis Assay. Steady-state velocity data were collected as described previously (37). Briefly, reactions containing 50 mM Tris (pH 8.1), 10 mM Mg(OAc)₂, 2 mM DTT, 150 mM NaCl (human Lon reactions only), and 200 nM Lon monomer in the presence and absence of 1.3 mM **1** or **2** ($\sim 5 \times K_m$) for *S. Typhimurium* Lon or 5 mM **1** ($\sim 5 \times K_m$) for human Lon were initiated by the addition of varying concentrations of [α -³²P]ATP (0–1 mM) and incubated at 37°C. At different time points (from 0 to 20 min), aliquots were quenched in 0.5 N formic acid. A 3 μL aliquot of each quenched reaction time point was spotted onto a PEI-cellulose TLC plate (10 cm \times 20 cm), and the plate developed in 0.3 M KPi (pH 3.4). The amount of [α -³²P]-ATP (ICN or Perkin-Elmer) and [α -³²P]ADP was quantified using a Packard Cyclone storage phosphor screen Phosphor imager (Perkin-Elmer Life Science), and the [ADP] generated was calculated using eq 2.

$$[\text{ADP}] = \left(\frac{\text{ADP}_{\text{dlu}}}{\text{ATP}_{\text{dlu}} + \text{ADP}_{\text{dlu}}} \right) [\text{ATP}] \quad (2)$$

The steady-state velocities were then determined from the linear phase of a plot of the amount of ADP generated versus time using KaleidaGraph (Synergy, Inc.). The steady-state kinetic parameters associated with ATP hydrolysis were determined by fitting the k_{obs} data with eq 3 using the nonlinear regression program Prism 4 (GraphPad Software, Inc.).

$$k_{\text{obs}} = \frac{k_{\text{cat}}[\text{S}]}{K_m + [\text{S}]} \quad (3)$$

where k_{obs} , k_{cat} , S , and K_m are as defined in eq 1. All experiments were performed at least in triplicate.

Mass Spectrometry of Peptide Cleavage Products. Reactions containing 50 mM Tris (pH 8.1), 10 mM Mg(OAc)₂, 2 mM DTT, 200 nM *S. Typhimurium* Lon monomer, and 100 μM peptide substrate were initiated by the addition of 1 mM ATP and incubated at 37°C. After 0 and 10 min, aliquots of the reactions mixture were quenched in 0.15% TFA final and submitted for MALDI mass spectrometry analysis (University of Cincinnati Mass Spectrometry Facility).

Determination of IC_{50} Values for Inhibitors. Experiments were performed as described under Continuous Steady-State Peptidase Activity Assay with the following modifications. All reactions contained 50 mM Tris (pH 8.1), 10 mM Mg(OAc)₂, 2 mM DTT, 300 nM *S. Typhimurium* Lon monomer, and 300 μM **2** (10% fluorescent/90% nonfluorescent, K_m level). Fifty seconds after initiation with 1 mM ATP, varying concentrations of the inhibitor (in 2 μL DMSO) were added. The time at which inhibitor was added was considered time zero. The steady-state velocities were determined from the

linear phase of the reaction time courses using KaleidaGraph (Synergy, Inc.). The IC_{50} under these conditions was determined by fitting the k_{obs} data with eq 4 (38).

$$\frac{k_{\text{obs},i}}{k_{\text{obs}}} = \frac{1}{1 + \frac{[\text{I}]}{\text{IC}_{50}}} \quad (4)$$

where $k_{\text{obs},i}$ is the observed rate constant in the presence of inhibitor, k_{obs} is the observed rate constant in the absence of inhibitor, I is inhibitor, and IC_{50} is the $[\text{I}]$ under which $k_{\text{obs},i}/k_{\text{obs}} = 0.5$. All experiments were performed in triplicate.

Determination of ATP Dependence of MG262 Inhibition. Steady-state velocity data were collected on a Fluoromax 3 spectrophotometer (Horiba Group) as previously described for *E. coli* Lon (35) with the following modifications. Reactions containing 50 mM Tris (pH 8.1), 10 mM Mg(OAc)₂, 2 mM DTT, and 300 nM *S. Typhimurium* Lon monomer were equilibrated for 1 min at 37°C prior to the addition of 1.2 μM MG262. At the times indicated, 1 mM ATP or AMPPNP and 300 μM **2** (10% fluorescent/90% nonfluorescent, K_m level) were added. The time at which **2** was added was considered time zero.

Estimation of K_i from IC_{50} Values. To approximate the K_i values for MG132, MG262, ethylboronic acid, and ZL₃OH, it was assumed that they were all competitive inhibitors of **2**. The IC_{50} values determined previously were used to estimate K_i using eq 5.

$$\text{IC}_{50} = K_i \left(1 + \frac{S_2}{K_{m,2}} \right) \quad (5)$$

where IC_{50} is as defined in eq 4, K_i is the inhibition constant, S_2 is the concentration of **2**, and $K_{m,2}$ is the Michaelis-Menten constant for **2**. To estimate the expected K_i for MG262 if it were simply a competitive, bivalent inhibitor made up of a peptide moiety (ZL₃OH) and a boronate moiety (ethylboronic acid), we used eqs 6–8 (39).

$$\Delta G_{\text{binding,ZL}_3\text{OH}} = RT \ln(K_{i,\text{ZL}_3\text{OH}}) \quad (6)$$

$$\Delta G_{\text{binding,ethyl}} = RT \ln(K_{i,\text{ethyl}}) \quad (7)$$

$$\Delta G_{\text{binding,MG262}} = \Delta G_{\text{binding,ZL}_3\text{OH}} + \Delta G_{\text{binding,ethyl}} = RT \ln(K_{i,\text{MG262}}) \quad (8)$$

where $\Delta G_{\text{binding,ZL}_3\text{OH}}$ is the free energy of binding for ZL₃OH, $K_{i,\text{ZL}_3\text{OH}}$ is the inhibition constant for ZL₃OH, $\Delta G_{\text{binding,ethyl}}$ is the free energy of binding for ethylboronic acid, $K_{i,\text{ethyl}}$ is the inhibition constant for ethylboronic acid, $\Delta G_{\text{binding,MG262}}$ is the estimated free energy of binding for MG262, and $K_{i,\text{MG262}}$ is the estimated inhibition constant for MG262.

RESULTS

Cloning and Purification of Recombinant Lon. The *S. Typhimurium* Lon gene was amplified from genomic DNA, cloned into the NcoI and HindIII sites of pET24d(+) (Novagen), and overexpressed in BL21 (DE3). The human Lon gene was amplified from proEx-1/hLon (34), cloned into the NdeI and BamHI sites of pET24c(+) (Novagen), and

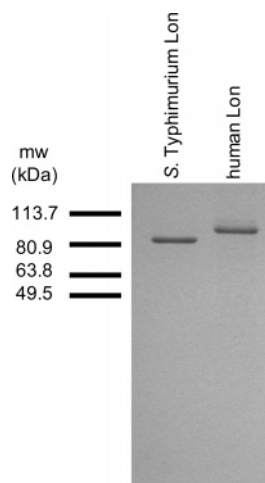


FIGURE 2: Coomassie stain of purified recombinant *S. Typhimurium* and human Lon. SDS-PAGE of ~365 ng of purified recombinant *S. Typhimurium* (87 kDa) and human Lon (95 kDa) visualized by Coomassie staining.

overexpressed in Rosetta (DE3). Both were purified to near homogeneity (Figure 2) as described in Materials and Methods. As much as 11 mg of *S. Typhimurium* Lon and 1.2 mg of human Lon can be purified from each liter of culture. The purified proteins are in their mature wild-type form and contain no exogenous tags, such as His or GST.

Steady-State Kinetic Analysis of Peptide Cleavage. We have previously developed a peptide substrate, **1**, for fluorescent detection of peptide cleavage by *E. coli* Lon (40). Upon cleavage, an increase in fluorescence is observed as the N-terminal 3-nitrotyrosine quencher separates from the C-terminal anthranilamide lysine fluorophore. We hypothesized that **1** could also be used to monitor proteolysis with recombinant *S. Typhimurium* and human Lon. In the absence of ATP, no peptide cleavage is observed, but in the presence of 1 mM ATP, *S. Typhimurium* and human Lon degrade **1** (Figure 3A). As with *E. coli* Lon, a lag is observed in peptide cleavage prior to reaching the steady-state activity (35).

We determined the steady-state kinetic constants associated with ATP-dependent degradation of **1** by *S. Typhimurium* and human Lon. The observed rate constants (k_{obs}) for steady-state cleavage of varying concentrations of **1** in the presence of saturating ATP were measured and plotted as a function of **1** (Figure 3B). Both give a sigmoidal plot, but the kinetic parameters for the two homologues are different (Table 1). *S. Typhimurium* Lon degrades **1** in a manner comparable to *E. coli* Lon (26, 35). Human Lon, on the other hand, has a similar degree of cooperativity (n), but k_{cat} is 2.5-fold lower and K_m is 5-fold greater than *S. Typhimurium* Lon (Table 1). This results in a k_{cat}/K_m for human Lon which is 10-fold lower than *S. Typhimurium* Lon (Table 1).

Our model peptide, **1**, contains a Cys residue (Figure 1), making its synthesis problematic due to the resulting low yield. The presence of a Cys residue in our substrate is also unfavorable as it will react with any thiol-reactive inhibitors. To avoid these problems, we changed the Cys to the non-natural amino acid Abu, which replaces the thiol by a methyl group and is therefore isosteric with Cys. The resultant peptide (**2**) was cleaved by *S. Typhimurium* Lon with steady-state kinetic parameters comparable to those for **1** (Table 1). Mass spectral analysis of the *S. Typhimurium* Lon

cleavage products of **1** and **2** verified that both peptides were cleaved at the same position (data not shown), as indicated in Figure 1.

To avoid the inner filter effect when determining the kinetic constants of peptide cleavage by the continuous peptide hydrolysis assay, mixtures of both fluorescent and nonfluorescent analogues of **1** and **2** were used. To rule out the possibility that the fluorescent and nonfluorescent analogues are degraded differently, the steady-state kinetic constants for peptide hydrolysis were also determined by a discontinuous peptide hydrolysis assay using only the fluorescent analogue. Similar kinetic constants were obtained using either assay (see Supporting Information).

Steady-State Kinetic Analysis of ATP Hydrolysis. ATP hydrolysis by Lon protease occurs in the absence of a substrate (intrinsic ATP hydrolysis) and is increased or stimulated in the presence of a peptide (40) or protein (8, 41) substrate (peptide- or protein-stimulated ATP hydrolysis, respectively). We determined the steady-state kinetic constants associated with ATP hydrolysis by recombinant *S. Typhimurium* and human Lon using a radiolabeled ATP hydrolysis assay (37). The k_{obs} values for steady-state ATP hydrolysis at varying concentrations of ATP both in the presence and absence of saturating **1** or **2** were measured and plotted as a function of ATP (Figure 4). Hyperbolic plots are obtained for both intrinsic and peptide-stimulated ATP hydrolysis by *S. Typhimurium* and human Lon. As expected, the intrinsic ATP hydrolysis activity of both homologues is stimulated by the presence of the peptide substrate. Similar kinetic constants for intrinsic and peptide-stimulated ATP hydrolysis are obtained irrespective of the homologue or peptide used (Table 2) and are comparable to those obtained previously with *E. coli* Lon (26).

Determination of IC_{50} Values for Common Proteasome Inhibitors. No potent or specific inhibitors of Lon protease activity are known. Because of the mechanistic and structural similarities between Lon and HslUV (26, 28, 42), the bacterial homologue of the proteasome, we screened a panel of commercially available peptide-based proteasome inhibitors to identify a lead compound, suitable for inhibiting Lon activity. Using *S. Typhimurium* Lon as a model, we determined the IC_{50} values for several proteasome inhibitors (Table 3) with respect to *S. Typhimurium* Lon proteolysis activity at 300 μM **2** (K_m level) and saturating ATP. Because of the lag phase, we did not add the inhibitor until after the steady-state was reached. MG132, a peptidyl aldehyde, inhibited *S. Typhimurium* Lon activity with an IC_{50} of $4.1 \pm 0.3 \mu\text{M}$. Epoxomicin, a peptidyl epoxyketone, and ZL₃-VS, a peptidyl vinyl sulfone, were ineffective at inhibiting *S. Typhimurium* Lon at micromolar concentrations (Table 3). All the proteasome inhibitors were dissolved in DMSO which did not affect *S. Typhimurium* Lon activity when it was less than 4% of the reaction volume (data not shown). Because of this limitation, the effect of higher concentrations of epoxomicin and ZL₃-VS could not be evaluated.

Most of the proteasome inhibitors were classical inhibitors of *S. Typhimurium* Lon activity, with inhibition occurring instantaneously upon addition. However, inhibition by MG262, a peptidyl boronate, was time-dependent or biphasic (Figure 5A). When calculating the IC_{50} for MG262 (Table 3), we used the rate of the second phase, as this was the final effect of inhibition. This resulted in an IC_{50} of $122 \pm$

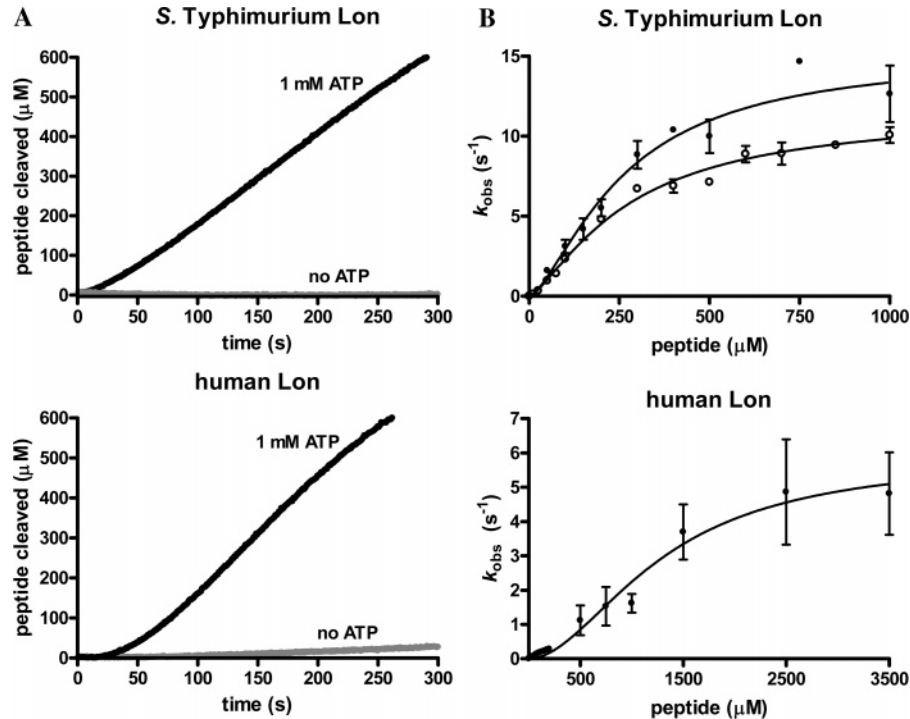


FIGURE 3: Steady-state peptide cleavage by *S. Typhimurium* and human Lon. (A) Representative time courses for *S. Typhimurium* (125 nM) and human (900 nM) Lon degradation of **1** (1 mM) in the presence and absence of ATP. (B) Reactions containing *S. Typhimurium* or human Lon were preincubated with varying concentrations of **1** (●) or **2** (○) prior to the addition of 1 mM ATP. All experiments were preformed at least in triplicate, and the averaged k_{obs} values (\pm 1 SD) were plotted against the corresponding peptide concentration. The data were best-fit with the Hill equation (eq 1) as described in Materials and Methods.

Table 1: Summary of Steady-State Kinetic Parameters for Peptide Hydrolysis

	<i>S. Typhimurium</i> Lon		human Lon
	1	2	1
k_{cat} (s ⁻¹)	15 \pm 2	11 \pm 1	5.9 \pm 0.7
K_m (μM)	262 \pm 61	276 \pm 38	1300 \pm 200
k_{cat}/K_m ($\times 10^3$ M ⁻¹ s ⁻¹)	57	40	4.5
n	1.5 \pm 0.3	1.4 \pm 0.2	1.9 \pm 0.3

9 nM for MG262 (Figure 5B), making it the most potent of all inhibitors tested.

Probing the Importance of the Peptide and Boronic Acid Moieties of MG262 in Inhibition. MG262 has both a peptide and boronic acid moiety, both of which are important for inhibiting the proteasome (43). To explore the contribution of each of these moieties toward inhibition of *S. Typhimurium* Lon activity, we determined the IC₅₀ for related compounds which resemble each moiety alone (Table 3). Ethylboronic acid and isopropylboronic acid were chosen as models for the boronic acid moiety of MG262. The IC₅₀ of ethylboronic acid could not be determined accurately due to solubility limitations, but was greater than 10 mM. Isopropylboronic acid, on the other hand, had an IC₅₀ of 810 \pm 50 μM (Figure 5C). We synthesized ZL₃OH (Table 3) as a model of the peptide moiety of MG262. The IC₅₀ of ZL₃OH was 740 \pm 29 μM (Figure 5D).

ATP-Dependent Inhibition of *S. Typhimurium* Lon by MG262. Previous work with *E. coli* Lon has shown that peptidyl chloromethyl ketones require ATP to inhibit Lon activity (8, 32). We wanted to know whether inhibition by MG262 also required ATP. To accomplish this, *S. Typhimurium* Lon was preincubated with MG262 for 0, 120, or 480 s. After the preincubation period, 1 mM ATP and 300

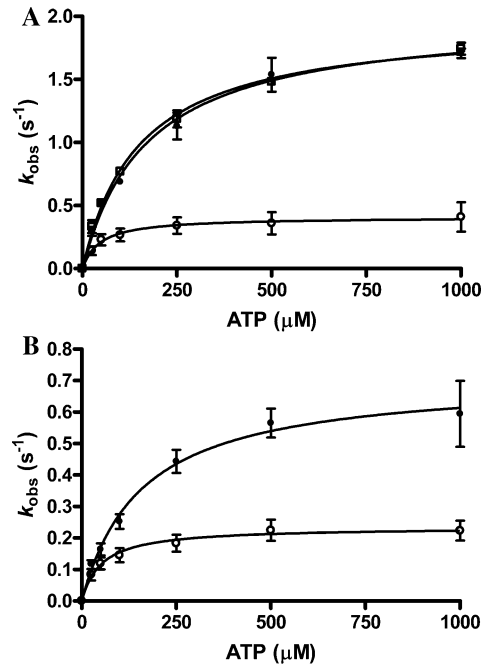


FIGURE 4: Steady-state ATP hydrolysis by *S. Typhimurium* and human Lon. Reactions containing *S. Typhimurium* (A) or human Lon (B) were preincubated in the absence (○) and presence of saturating ($\sim 5 \times K_m$) **1** (●) or **2** (□) prior to the addition of varying concentrations of ATP. All experiments were preformed at least in triplicate, and the averaged k_{obs} values (\pm 1 SD) were plotted against the corresponding ATP concentration. The data were best-fit with the Michaelis–Menten equation as described in Materials and Methods.

μM **2** were added and peptide cleavage monitored over 600 s (Figure 6A). No differences in the time courses were observed, indicating that inhibition by MG262 did not begin

Table 2: Summary of Steady-State Kinetic Parameters for ATP Hydrolysis

	<i>S. Typhimurium</i> Lon			Human Lon	
	intrinsic	1 stimulated	2 stimulated	intrinsic	1 stimulated
k_{cat} (s^{-1})	0.41 ± 0.05	2.0 ± 0.1	2.0 ± 0.1	0.23 ± 0.02	0.71 ± 0.06
K_m (μM)	46 ± 24	172 ± 24	150 ± 12	52 ± 17	158 ± 39

until the addition of ATP and **2**. *S. Typhimurium* Lon was then preincubated with MG262 and ATP for 0, 120, or 480 s. After the preincubation period, **2** was added and peptide cleavage again monitored over 600 s (Figure 6B). As the length of the preincubation period was increased, time dependency was lost. In fact, preincubation for 480 s resulted in a total loss of time dependency. Control reactions were performed in which MG262 was omitted (DMSO only). The presence of ATP alone during the preincubation period did not affect the rate of peptide hydrolysis; thus, the loss of time dependency was the direct result of inhibition by MG262 and not ATP depletion or ADP inhibition (data not shown). Regardless of the length of the preincubation period, the final steady-state rates were identical (29 ± 6 nM/s).

It has previously been shown that *E. coli* Lon requires binding, but not hydrolysis, of ATP in order to cleave a peptide substrate, albeit at a reduced rate (35). To determine whether inhibition by MG262 required both binding and hydrolysis of ATP, we repeated the latter experiment (preincubation with MG262 and nucleotide) with 1 mM AMPPNP (Figure 6C). The same trend was observed with AMPPNP as with ATP. Time dependency was lost as the preincubation period was increased, and the steady-state rates were identical regardless of the preincubation time (34 ± 5 nM/s). Control reactions were again performed without MG262 (DMSO only), and peptide hydrolysis was not affected by the presence of AMPPNP during the preincubation period (data not shown); thus, the observed trend was the direct result of inhibition by MG262.

DISCUSSION

Lon protease is an ATP-dependent serine protease and has emerged as a target in the development of novel antibiotics. To date, no potent or specific inhibitors of this enzyme have been described. In this study, we use steady-state kinetic techniques to quantitatively evaluate a series of commercially available inhibitors in order to identify a lead compound for future development of a bacterial Lon-specific inhibitor.

Lon catalyzes the hydrolysis of both ATP and proteins within different domains, presenting two possible approaches in developing Lon inhibitors. We evaluated the steady-state kinetic parameters for peptide and ATP hydrolysis to investigate which approach would allow an inhibitor to discriminate between *S. Typhimurium* and human Lon. The parameters associated with ATP-hydrolysis are similar for both (Table 2); however, the catalytic efficiency (k_{cat}/K_m) of peptide degradation by human Lon is 10-fold lower than *S. Typhimurium* Lon (Table 1). This implies there is a difference in the substrate specificity of the two homologues. This is not unexpected, as the two localize differently and would degrade a vastly different protein pool (8, 16). We conclude that a peptide-based approach to develop an inhibitor would be more useful, as the observed difference in substrate

specificity could potentially be exploited to target an inhibitor specifically to bacterial Lon, thereby decreasing the chance for side-effects resulting from cross-reactivity with the human homologue.

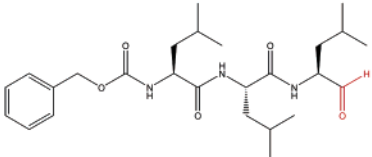
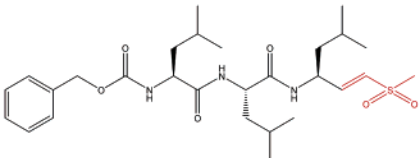
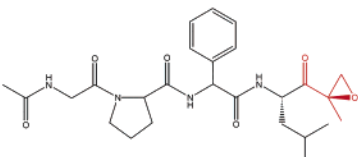
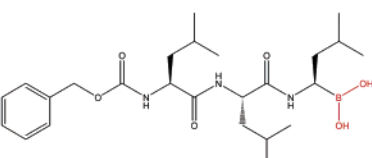
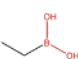
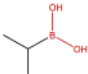
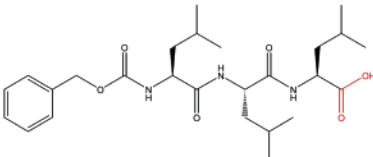
Lon is unique in that, while classified as a serine protease, it is susceptible to both serine and cysteine protease inhibitors (30–32). Of the soluble ATP-dependent proteases within the AAA⁺ superfamily, Lon more closely resembles proteases within the proteasome family (26, 27, 29, 42). As such, we began our search for a Lon inhibitor by screening a series of commercially available peptide-based proteasome inhibitors. In choosing inhibitors for our screen, we attempted to choose those containing similar peptide sequences, with only the reactive functional group varying. In this way, we could still evaluate the ability of each functional group to inhibit Lon without the need to synthesize a new series of inhibitors. Using a standard set of conditions, 300 μM **2** (K_m level), 300 nM *S. Typhimurium* Lon, and saturating ATP, we determined the IC_{50} for each inhibitor in our series (Table 3).

Peptidyl vinyl sulfones were designed to inhibit cysteine proteases via Michael addition (44); however, they were later shown to react with both serine and threonine proteases (45–48). We tested the peptidyl vinyl sulfone ZL₃VS as an inhibitor of *S. Typhimurium* Lon activity, but it did not appear to have any inhibitory effect (Table 3). The reason for the lack of inhibition is unclear. We believe this indicates the orientation of the active site residues, with respect to the peptide binding pocket, are different between the proteasome and Lon, thereby misaligning the vinyl sulfone for nucleophilic attack.

The natural product epoxomicin, a peptidyl epoxyketone, is the most selective proteasome inhibitor known due to its unique mechanism of inhibition (49, 50). The final covalent adduct is a morpholino ring which contains not only the Thr hydroxyl, but also the N-terminal amino group (51). The crystal structure of the protease domain of *E. coli* Lon was determined with a proteolytically inactive mutant; thus, the orientation of the nucleophilic hydroxyl group is unknown, as well as how this hydroxyl affects the orientation of the ϵ -amino group of the proposed Ser–Lys dyad (42). We hypothesized that if the Ser–Lys dyad of Lon was indeed analogous to the catalytic dyad of the proteasome, epoxomicin inhibition of Lon would provide further insight into the orientation of these residues. Unfortunately, epoxomicin was unable to inhibit *S. Typhimurium* Lon (Table 3). Thus, we are able only to conclude that the orientation of the active site residues of both Lon and the proteasome is different. This result reinforces the unique specificity of epoxomicin for the proteasome.

Peptidyl aldehydes and boronates were designed to function as transition state analogue inhibitors of proteolytic enzymes, with an active site thiol or hydroxyl, via formation of a tetrahedral adduct (43, 52–55). Peptidyl aldehydes inhibit cysteine, serine, and threonine proteases effectively, with some preference for cysteine due to the higher nucleophilicity of the thiol. Peptidyl boronates, on the other hand, are much more potent against serine and threonine proteases due to the weakness of the boron–sulfur bond in the covalent adduct with cysteine (43). MG132, a peptidyl aldehyde, and MG262, a peptidyl boronate, both inhibit *S. Typhimurium* Lon, with IC_{50} values of 4.1 ± 0.3 μM and 122 ± 9 nM,

Table 3: Summary of IC_{50} Values for Inhibition of *S. Typhimurium* Lon

inhibitor	functionality/structure	IC_{50} (μ M)
	aldehyde	
MG132		4.1 ± 0.3
	vinyl sulfone	
ZL ₃ VS		> 167
	epoxyketone	
epoxomicin		> 200
	boronate	
MG262		0.122 ± 0.009
	boronate	
ethylboronic acid		> 10000
	boronate	
isopropylboronic acid		810 ± 50
	carboxylate	
ZL ₃ OH		740 ± 29

respectively (Table 3, Figure 5B). The K_i value for each can be estimated from the IC_{50} value (2μ M for MG132, 60 nM for MG262) as described under Materials and Methods (39). Although these are some of the best inhibitors of Lon known to date, both are ~ 2000 -fold more potent against the 20S proteasome (43). This weaker reactivity of MG132 and MG262 toward *S. Typhimurium* Lon may imply the local environment of the active site renders the hydroxyl less nucleophilic than in the proteasome and/or the peptide sequence is not optimal for binding to Lon. It is clear that transition state analogues will be useful in the development of more potent inhibitors of Lon activity.

Our best inhibitor, MG262, has both a peptide and boronic acid moiety, both of which are important for inhibition of the 20S proteasome (43). To determine the importance of each of these moieties in *S. Typhimurium* Lon inhibition, we determined the IC_{50} values for compounds representing each moiety separately. To model the boronate moiety alone, we chose both ethyl- and isopropylboronic acid. The IC_{50} of ethylboronic acid was $> 10 \text{ mM}$; however, the IC_{50} for isopropylboronic was $810 \pm 50 \mu\text{M}$ (Table 3, Figure 5C). The observed difference in IC_{50} for the two compounds is unknown; however, we speculate that the larger alkyl group may help anchor the boronic acid in the active site, thereby

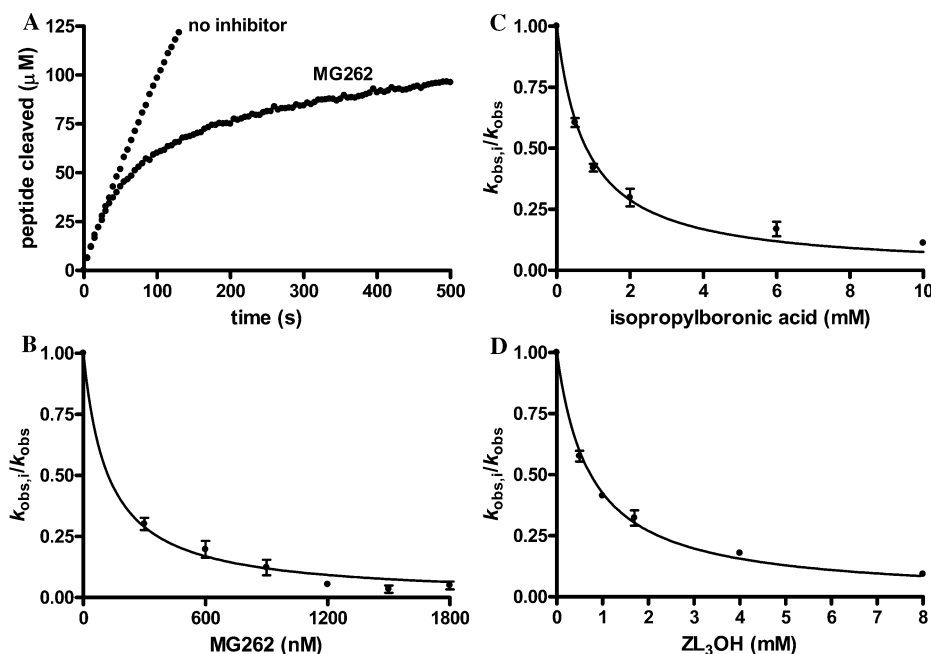


FIGURE 5: Inhibition of *S. Typhimurium* Lon degradation of **2**. (A) Representative time courses for *S. Typhimurium* Lon (300 nM) degradation of **2** (300 μ M, K_m level) in the absence and presence of MG262 (0.9 μ M). (B–D) Reactions containing 300 nM *S. Typhimurium* Lon were preincubated with 300 μ M **2** (K_m level) prior to the addition of 1 mM ATP. After 50 s, 2 μ L of inhibitor in DMSO was added and peptide cleavage monitored over 550 s. All experiments were performed in triplicate and the k_{obs} values determined as described in Materials and Methods. The averaged k_{obs} in the presence of inhibitor/ k_{obs} in the absence of inhibitor ($k_{obs,i}/k_{obs}$, ± 1 SD) were plotted against the corresponding inhibitor concentration. The IC_{50} for each inhibitor was determined by fitting the data as described in Materials and Methods. Inhibition by MG262 (B) resulted in an $IC_{50} = 122 \pm 9$ nM, inhibition by isopropylboronic acid (C) yielded an $IC_{50} = 810 \pm 50$ μ M, and inhibition by ZL₃OH resulted in an $IC_{50} = 740 \pm 29$ μ M.

facilitating inhibition. We also synthesized the peptide ZL₃-OH as a mimic of the peptide moiety of MG262 and found it had an IC_{50} of 740 ± 29 μ M (Table 3, Figure 5D). Neither the boronate nor peptide alone could achieve the nanomolar potency found for MG262. We can again approximate the K_i using the IC_{50} values, as described under Material and Methods, and obtain 5 mM for ethylboronic acid and 400 μ M for ZL₃OH (39). If we consider MG262 a bivalent inhibitor made up of the boronate and peptide moieties, we would, at best, expect an IC_{50} of ~ 4 μ M (39). In reality, MG262 is actually 30-fold more potent (Table 3), indicating the inhibition is more complicated than simply increased affinity and will require further investigation.

Inhibition of *E. coli* Lon by peptidyl chloromethyl ketones requires ATP (8, 32); therefore, we suspected that MG262 may also require ATP for inhibition. Preincubation of MG262 with *S. Typhimurium* Lon for varying lengths of time in the absence of ATP did not affect the degradation of **2** (Figure 6A). In the presence of ATP, as the preincubation time was increased, time-dependency was lost (Figure 6B); however, the steady-state rates remained the same (29 ± 6 nM/s). Looking at the time course with no preincubation period (0 s, Figure 6B), we see that after 480 s, *S. Typhimurium* Lon has achieved steady-state turnover. If the presence of ATP during the preincubation period allowed for the formation of the MG262-inhibited species, we would predict that preincubation for 480s would be enough time for maximal inhibition to occur. Thus, upon the addition of **2**, no time dependency would be expected and the linear plot should have a steady-state rate which matches that for no preincubation. This is exactly what we observe (480 s, Figure 6B). Time dependency only appears to be lost because less active *S. Typhimurium* Lon is available upon the addition

of **2**. The time-dependent inactivation occurs during the preincubation period. The ATP-dependence of MG262 inhibition of *S. Typhimurium* Lon is of mechanistic importance. It implies MG262 is a mechanism-based inhibitor of Lon and that inhibitors cannot simply diffuse into the active site; the ATP is required to deliver the inhibitor to the active site. Inhibition of HslUV by peptide-based inhibitors also requires ATP, further supporting our use of HslUV as a model for Lon (45).

To investigate whether MG262 inhibition required both binding and hydrolysis of ATP, we preincubated *S. Typhimurium* Lon with MG262 and the nonhydrolyzable ATP analogue AMPPNP for varying lengths of time. If only ATP binding was required, we would again expect to see an apparent loss of time dependency as the preincubation time is increased, but the steady-state rate remain constant. From Figure 6C, we see that this trend is indeed obtained (steady-state rate = 34 ± 5 nM/s). Thus, MG262 inhibition requires only ATP binding and not hydrolysis.

On the basis of the data obtained during this study, we propose the following mechanism (Scheme 1) to account for MG262 inhibition of *S. Typhimurium* Lon. First, the substrates must bind to *S. Typhimurium* Lon, creating a ternary complex (Scheme 1, step 1). It has previously been shown that ATP binding induces a conformational change in both *E. coli* Lon and HslUV and that, in HslUV, this conformational change results in the productive alignment of the substrate with the active site Thr of HslUV (26, 46, 56). On the basis of these observations, we believe *S. Typhimurium* Lon next undergoes a conformational change (Lon*) within the ternary complex as a result of ATP binding (Scheme 1, step 2). This conformational change correctly aligns the boronate moiety of MG262 for nucleophilic attack by the

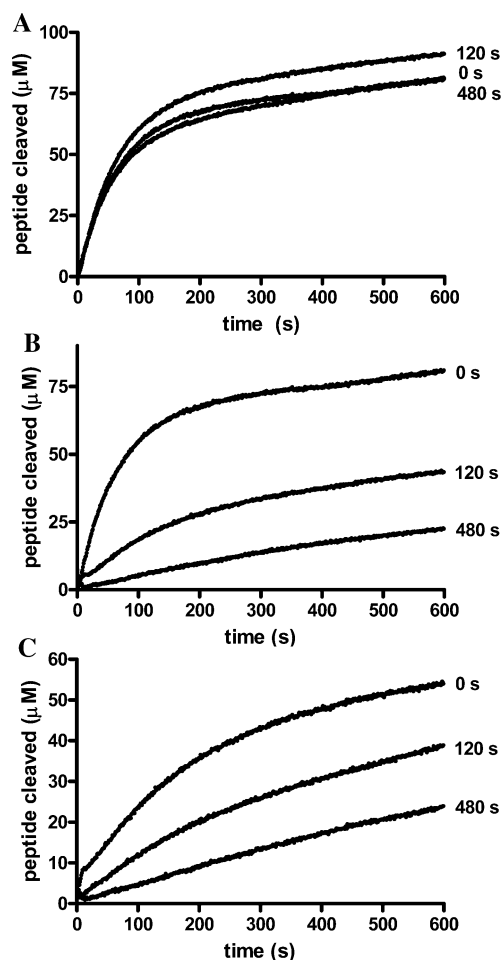
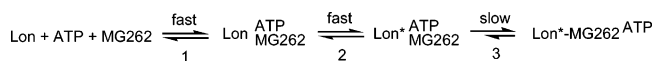


FIGURE 6: MG262 inhibition of *S. Typhimurium* Lon requires ATP. Reactions containing 300 nM *S. Typhimurium* Lon were preincubated with 1.2 μ M MG262 (A), 1.2 μ M MG262 and 1 mM ATP (B), or 1.2 μ M MG262 and 1 mM AMPNP prior to the addition of 300 μ M 2 and 1 mM ATP (A only) after the indicated time. Peptide cleavage was monitored over 600 s. All experiments were performed in triplicate and the averaged time courses plotted against time.

Scheme 1



- 1 - substrate binding
2 - conformational change
3 - covalent modification

active site Ser. It is only at this point that covalent modification of *S. Typhimurium* Lon by MG262 (Lon*-MG262) occurs to give the final inhibited binary species (Scheme 1, step 3). Although the covalent modification is reversible, the equilibrium would lie toward the covalently modified species (unpublished data), which is consistent with MG262 inhibition of the 20S proteasome (33). The first two steps appear to be fast, as inhibition by ZL₅OH occurs immediately upon addition (i.e., it is a classical inhibitor) (data not shown). We believe the last step is slow due to the observation of time-dependent inhibition by MG262 (Figure 5A). Further studies are currently underway to determine these details and confirm the proposed mechanism.

In this study, we have shown that bacterial and human Lon display differences in substrate specificity which may be exploited in the future to discriminate between the

homologues. We have demonstrated the use of a peptidyl boronic acid, MG262, as a potent ATP-dependent inhibitor of *S. Typhimurium* Lon activity. It should be noted that proteasome inhibitors, such as MG132, are able to diffuse into the mitochondria and inhibit the degradation of the steroidogenic acute regulatory protein (StAR), a physiological substrate of mammalian Lon (57, 58). It has also been shown that the proteasome inhibitor bortezomib, a peptidyl boronate currently used in the treatment of multiply myeloma, causes mitochondrial damage by an unknown mechanism (59, 60). Thus, it is imperative that detailed kinetic analysis of the inhibition profile of human Lon by these peptide-based inhibitors be performed, as well as determination of the mechanism by which these inhibitors affect Lon activity, so that cross-reactivity with other proteases, and other homologues of Lon, is minimized.

ACKNOWLEDGMENT

We would like to thank Diana Vineyard, Jessica Ward, and Xuemei Zhang for their assistance in preparing this manuscript.

SUPPORTING INFORMATION AVAILABLE

Details of the discontinuous steady-state peptide hydrolysis assay and figure of steady-state cleavage by *S. Typhimurium* and human Lon. This material is available free of charge via the Internet at <http://pubs.acs.org>.

REFERENCES

- Monaghan, R. L., and Barrett, J. F. (2006) Antibacterial drug discovery—then, now and the genomics future, *Biochem. Pharmacol.* **71**, 901–909.
- Robertson, G. T., Kovach, M. E., Allen, C. A., Ficht, T. A., and Roop, R. M., II (2000) The *Brucella abortus* Lon functions as a generalized stress response protease and is required for wild-type virulence in BALB/c mice, *Mol. Microbiol.* **35**, 577–588.
- Takaya, A., Suzuki, M., Matsui, H., Tomoyasu, T., Sashinami, H., Nakane, A., and Yamamoto, T. (2003) Lon, a stress-induced ATP-dependent protease, is critically important for systemic *Salmonella enterica* serovar typhimurium infection of mice, *Infect. Immun.* **71**, 690–696.
- Matsui, H., Suzuki, M., Isshiki, Y., Kodama, C., Eguchi, M., Kikuchi, Y., Motokawa, K., Takaya, A., Tomoyasu, T., and Yamamoto, T. (2003) Oral immunization with ATP-dependent protease-deficient mutants protects mice against subsequent oral challenge with virulent *Salmonella enterica* serovar typhimurium, *Infect. Immun.* **71**, 30–39.
- Charette, M. F., Henderson, G. W., Doane, L. L., and Markovitz, A. (1984) DNA-stimulated ATPase activity on the lon (CapR) protein, *J. Bacteriol.* **158**, 195–201.
- Chung, C. H., and Goldberg, A. L. (1981) The product of the lon (capR) gene in *Escherichia coli* is the ATP-dependent protease, protease La, *Proc. Natl. Acad. Sci. U.S.A.* **78**, 4931–4935.
- Goff, S. A., and Goldberg, A. L. (1985) Production of abnormal proteins in *E. coli* stimulates transcription of lon and other heat shock genes, *Cell* **41**, 587–595.
- Goldberg, A. L., Moerschell, R. P., Chung, C. H., and Maurizi, M. R. (1994) ATP-dependent protease La (lon) from *Escherichia coli*, *Methods Enzymol.* **244**, 350–375.
- Goldberg, A. L., and Waxman, L. (1985) The role of ATP hydrolysis in the breakdown of proteins and peptides by protease La from *Escherichia coli*, *J. Biol. Chem.* **260**, 12029–12034.
- Gottesman, S. (1996) Proteases and their targets in *Escherichia coli*, *Annu. Rev. Genet.* **30**, 465–506.
- Gottesman, S., Gottesman, M., Shaw, J. E., and Pearson, M. L. (1981) Protein degradation in *E. coli*: the lon mutation and bacteriophage lambda N and cII protein stability, *Cell* **24**, 225–233.

12. Gottesman, S., and Maurizi, M. R. (1992) Regulation by proteolysis: energy-dependent proteases and their targets, *Microbiol. Rev.* **56**, 592–621.
13. Maurizi, M. R. (1992) Proteases and protein degradation in *Escherichia coli*, *Experientia* **48**, 178–201.
14. Schoemaker, J. M., Gayda, R. C., and Markovitz, A. (1984) Regulation of cell division in *Escherichia coli*: SOS induction and cellular location of the *sulA* protein, a key to lon-associated filamentation and death, *J. Bacteriol.* **158**, 551–561.
15. Suzuki, C. K., Kutejova, E., and Suda, K. (1995) Analysis and purification of ATP-dependent mitochondrial lon protease of *Saccharomyces cerevisiae*, *Methods Enzymol.* **260**, 486–494.
16. Wang, N., Maurizi, M. R., Emmert-Buck, L., and Gottesman, M. M. (1994) Synthesis, processing, and localization of human Lon protease, *J. Biol. Chem.* **269**, 29308–29313.
17. Huang, X., and Miller, W. (1991) A time-efficient, linear-space local similarity algorithm, *Adv. Appl. Math.* **12**, 337–357.
18. Apte, B. N., Rhodes, H., and Zipser, D. (1975) Mutation blocking the specific degradation of reinitiation polypeptides in *E. coli*, *Nature* **257**, 329–331.
19. Downs, D., Waxman, L., Goldberg, A. L., and Roth, J. (1986) Isolation and characterization of lon mutants in *Salmonella typhimurium*, *J. Bacteriol.* **165**, 193–197.
20. Gottesman, S., and Zipser, D. (1978) Deg phenotype of *Escherichia coli* lon mutants, *J. Bacteriol.* **133**, 844–851.
21. Grossman, A. D., Burgess, R. R., Walter, W., and Gross, C. A. (1983) Mutations in the *lon* gene of *E. coli* K12 phenotypically suppress a mutation in the sigma subunit of RNA polymerase, *Cell* **32**, 151–159.
22. Howard-Flanders, P., Simson, E., and Theriot, L. (1964) A locus that controls filament formation and sensitivity to radiation in *Escherichia coli* K-12, *Genetics* **49**, 237–246.
23. Mizusawa, S., and Gottesman, S. (1983) Protein degradation in *Escherichia coli*: the *lon* gene controls the stability of *sulA* protein, *Proc. Natl. Acad. Sci. U.S.A.* **80**, 358–362.
24. Dougan, D. A., Mogk, A., Zeth, K., Turgay, K., and Bukau, B. (2002) AAA⁺ proteins and substrate recognition, it all depends on their partner in crime, *FEBS Lett.* **529**, 6–10.
25. Patel, S., and Latterich, M. (1998) The AAA team: related ATPases with diverse functions, *Trends Cell Biol.* **8**, 65–71.
26. Patterson, J., Vineyard, D., Thomas-Wohlever, J., Behshad, R., Burke, M., and Lee, I. (2004) Correlation of an adenine-specific conformational change with the ATP-dependent peptidase activity of *Escherichia coli* Lon, *Biochemistry* **43**, 7432–7442.
27. Wang, J., Song, J. J., Seong, I. S., Franklin, M. C., Kamtekar, S., Eom, S. H., and Chung, C. H. (2001) Nucleotide-dependent conformational changes in a protease-associated ATPase HslU, *Structure (Cambridge, MA, U.S.)* **9**, 1107–1116.
28. Botos, I., Melnikov, E. E., Cherry, S., Khalatova, A. G., Rasulova, F. S., Tropea, J. E., Maurizi, M. R., Rotanova, T. V., Gustchina, A., and Wlodawer, A. (2004) Crystal structure of the AAA⁺ alpha domain of *E. coli* Lon protease at 1.9 Å resolution, *J. Struct. Biol.* **146**, 113–122.
29. Lowe, J., Stock, D., Jap, B., Zwickl, P., Baumeister, W., and Huber, R. (1995) Crystal structure of the 20S proteasome from the archaeon *T. acidophilum* at 3.4 Å resolution, *Science* **268**, 533–539.
30. Bota, D. A., and Davies, K. J. (2002) Lon protease preferentially degrades oxidized mitochondrial aconitase by an ATP-stimulated mechanism, *Nat. Cell Biol.* **4**, 674–680.
31. Waxman, L., and Goldberg, A. L. (1982) Protease La from *Escherichia coli* hydrolyzes ATP and proteins in a linked fashion, *Proc. Natl. Acad. Sci. U.S.A.* **79**, 4883–4887.
32. Waxman, L., and Goldberg, A. L. (1985) Protease La, the lon gene product, cleaves specific fluorogenic peptides in an ATP-dependent reaction, *J. Biol. Chem.* **260**, 12022–12028.
33. Kisselev, A. F., and Goldberg, A. L. (2001) Proteasome inhibitors: from research tools to drug candidates, *Chem. Biol.* **8**, 739–758.
34. Fu, G. K., and Markovitz, D. M. (1998) The human LON protease binds to mitochondrial promoters in a single-stranded, site-specific, strand-specific manner, *Biochemistry* **37**, 1905–1909.
35. Thomas-Wohlever, J., and Lee, I. (2002) Kinetic characterization of the peptidase activity of *Escherichia coli* Lon reveals the mechanistic similarities in ATP-dependent hydrolysis of peptide and protein substrates, *Biochemistry* **41**, 9418–9425.
36. Liu, T., Lu, B., Lee, I., Ondrovicova, G., Kutejova, E., and Suzuki, C. K. (2004) DNA and RNA binding by the mitochondrial lon protease is regulated by nucleotide and protein substrate, *J. Biol. Chem.* **279**, 13902–13910.
37. Gilbert, S. P., and Mackey, A. T. (2000) Kinetics: a tool to study molecular motors, *Methods* **22**, 337–354.
38. Copeland, R. A. (2000) *Enzymes: A Practical Introduction to Structure, Mechanism, and Data Analysis*, 2nd ed., John Wiley & Sons, Inc., New York.
39. Copeland, R. A. (2005) *Evaluation of Enzyme Inhibitors in Drug Discovery: A Guide for Medicinal Chemists and Pharmacologists*, John Wiley & Sons, Inc., Hoboken, NJ.
40. Lee, I., and Berdis, A. J. (2001) Adenosine triphosphate-dependent degradation of a fluorescent lambda N substrate mimic by Lon protease, *Anal. Biochem.* **291**, 74–83.
41. Waxman, L., and Goldberg, A. L. (1986) Selectivity of intracellular proteolysis: protein substrates activate the ATP-dependent protease (La), *Science* **232**, 500–503.
42. Botos, I., Melnikov, E. E., Cherry, S., Tropea, J. E., Khalatova, A. G., Rasulova, F., Dauter, Z., Maurizi, M. R., Rotanova, T. V., Wlodawer, A., and Gustchina, A. (2004) The catalytic domain of *Escherichia coli* Lon protease has a unique fold and a Ser-Lys dyad in the active site, *J. Biol. Chem.* **279**, 8140–8148.
43. Adams, J., Behnke, M., Chen, S., Cruickshank, A. A., Dick, L. R., Grenier, L., Klunder, J. M., Ma, Y. T., Plamondon, L., and Stein, R. L. (1998) Potent and selective inhibitors of the proteasome: dipeptidyl boronic acids, *Bioorg. Med. Chem. Lett.* **8**, 333–338.
44. Palmer, J. T., Rasnick, D., Klaus, J. L., and Bromme, D. (1995) Vinyl sulfones as mechanism-based cysteine protease inhibitors, *J. Med. Chem.* **38**, 3193–3196.
45. Bogoy, M., McMaster, J. S., Gaczynska, M., Tortorella, D., Goldberg, A. L., and Ploegh, H. (1997) Covalent modification of the active site threonine of proteasomal beta subunits and the *Escherichia coli* homolog HslV by a new class of inhibitors, *Proc. Natl. Acad. Sci. U.S.A.* **94**, 6629–6634.
46. Sousa, M. C., Kessler, B. M., Overkleeft, H. S., and McKay, D. B. (2002) Crystal structure of HslUV complexed with a vinyl sulfone inhibitor: corroboration of a proposed mechanism of allosteric activation of HslV by HslU, *J. Mol. Biol.* **318**, 779–785.
47. Joyeau, R., Maoulida, C., Guillet, C., Frappier, F., Teixeira, A. R., Schrevel, J., Santana, J., and Grellier, P. (2000) Synthesis and activity of pyrrolidinyl- and thiazolidinyl-dipeptide derivatives as inhibitors of the Tc80 prolyl oligopeptidase from *Trypanosoma cruzi*, *Eur. J. Med. Chem.* **35**, 257–266.
48. Bogoy, M., Shin, S., McMaster, J. S., and Ploegh, H. L. (1998) Substrate binding and sequence preference of the proteasome revealed by active-site-directed affinity probes, *Chem. Biol.* **5**, 307–320.
49. Meng, L., Mohan, R., Kwok, B. H., Elofsson, M., Sin, N., and Crews, C. M. (1999) Epoxomicin, a potent and selective proteasome inhibitor, exhibits in vivo antiinflammatory activity, *Proc. Natl. Acad. Sci. U.S.A.* **96**, 10403–10408.
50. Hanada, M., Sugawara, K., Kaneta, K., Toda, S., Nishiyama, Y., Tomita, K., Yamamoto, H., Konishi, M., and Oki, T. (1992) Epoxomicin, a new antitumor agent of microbial origin, *J. Antibiot. (Tokyo)* **45**, 1746–1752.
51. Groll, M., Kim, K. B., Kairies, N., Huber, R., and Crews, C. M. (2000) Crystal structure of epoxomicin: 20S proteasome reveals a molecular basis for selectivity of α' - β' -epoxyketone proteasome inhibitors, *J. Am. Chem. Soc.* **122**, 1237–1238.
52. Koehler, K. A., and Lienhard, G. E. (1971) 2-Phenylethaneboronic acid, a possible transition-state analog for chymotrypsin, *Biochemistry* **10**, 2477–2483.
53. Thompson, R. C. (1973) Use of peptide aldehydes to generate transition-state analogs of elastase, *Biochemistry* **12**, 47–51.
54. Westerik, J. O., and Wolfenden, R. (1972) Aldehydes as inhibitors of papain, *J. Biol. Chem.* **247**, 8195–8197.
55. Vinitsky, A., Michaud, C., Powers, J. C., and Orłowski, M. (1992) Inhibition of the chymotrypsin-like activity of the pituitary multicatalytic proteinase complex, *Biochemistry* **31**, 9421–9428.
56. Yoo, S. J., Kim, H. H., Shin, D. H., Lee, C. S., Seong, I. S., Seol, J. H., Shimbara, N., Tanaka, K., and Chung, C. H. (1998) Effects of the cys mutations on structure and function of the ATP-dependent HslVU protease in *Escherichia coli*. The Cys287 to Val mutation in HslU uncouples the ATP-dependent proteolysis by HslVU from ATP hydrolysis, *J. Biol. Chem.* **273**, 22929–22935.
57. Granot, Z., Geiss-Friedlander, R., Melamed-Book, N., Eimerl, S., Timberg, R., Weiss, A. M., Hales, K. H., Hales, D. B., Stocco, D. M., and Orly, J. (2003) Proteolysis of normal and mutated

- steroidogenic acute regulatory proteins in the mitochondria: the fate of unwanted proteins, *Mol. Endocrinol.* **17**, 2461–2476.
58. Ondrovicova, G., Liu, T., Singh, K., Tian, B., Li, H., Gakh, O., Perecko, D., Janata, J., Granot, Z., Orly, J., Kutejova, E., and Suzuki, C. K. (2005) Cleavage site selection within a folded substrate by the ATP-dependent lon protease, *J. Biol. Chem.* **280**, 25103–25110.
59. Ling, Y. H., Liebes, L., Zou, Y., and Perez-Soler, R. (2003) Reactive oxygen species generation and mitochondrial dysfunction in the apoptotic response to Bortezomib, a novel proteasome inhibitor, in human H460 non-small cell lung cancer cells, *J. Biol. Chem.* **278**, 33714–33723.
60. Pei, X. Y., Dai, Y., and Grant, S. (2003) The proteasome inhibitor bortezomib promotes mitochondrial injury and apoptosis induced by the small molecule Bcl-2 inhibitor HA14–1 in multiple myeloma cells, *Leukemia* **17**, 2036–2045.

BI060542E